

# Remote temperature mapping of high-power InGaN/GaN MQW flip-chip design LEDs

V.K. Malyutenko<sup>1</sup>, O.Yu. Malyutenko, A.V. Zinovchuk  
Institute of Semiconductor Physics, Kiev, Ukraine  
A.L. Zakheim, D.A. Zakheim, I.P. Smirnova, S.A. Gurevich  
Ioffe Physico-Technical Institute, St. Petersburg, Russia

## ABSTRACT

We report on the study of heat 2D-distribution in InGaN LEDs with the stress made on local device overheating and temperature gradients inside the structure. The MQW InGaN/GaN/sapphire blue LEDs are designed as bottom emitting devices where light escapes the structure through the transparent GaN current spreading layer and sapphire substrate, whereas the LED structure with high-reflectivity Ni/Ag p-contact is bonded to the thermally conductive Si submount by a flip-chip method. The measurements are performed with an IR microscope operating in a time-resolved mode (3-5  $\mu\text{m}$  spectral range,  $<20 \mu\text{m}$  spatial and  $10 \mu\text{s}$  temporal resolution), while scanning a heat emission map through a transparent sapphire substrate. We show how current crowding (which is difficult to avoid) causes a local hot region near the n-contact pads and affects the performance of the device at a high injection level.

**Keywords:** nitrides, multiple quantum wells, blue LEDs, IR microscopy, temperature micro mapping

## 1. INTRODUCTION

The GaN-based visible LEDs grown on sapphire substrates are already in the market for a decade. It is believed that these devices grown as heterostructures with single or multiple quantum wells (MQW) provide higher performance in the short-wavelength (380-520nm) part of the visible spectrum compared to any other materials system. In the recent years, research on (Al, In)GaN LEDs pivots around high power characteristics, the most important of which are higher CW output power, enhanced wall-plug efficiency, lower thermal resistance, long lifetime, and low lumens cost (\$/lm). Among several approaches to develop a device with improved performance, it is the flip-chip technique that satisfies most of above-mentioned demands. In this design, to bypass heat transfer through low thermal conductivity sapphire substrate and better extract a light beam, p-n junction positions close to a heat sink and light escapes the structure through a transparent GaN current spreading layer and a sapphire substrate.

Although flip-chip technology is now emerging as the most effective way to design high-power GaN-based LEDs, the p-n junction overheating and non-uniform heat dissipation through a device structure affect CW operation at an extreme mode and cause premature device degradation. Because of their wide bandgap and low intrinsic carrier concentration, nitrides generally permit high temperature operation (up to  $T=200^\circ\text{C}$ <sup>1</sup>). However, these devices typically show a large decrease in quantum efficiency and lifetime with increasing operating current. Therefore, the crucial issue is the role of overheating in output power saturation and degradation processes at a high excitation level. As a matter of fact, thermal management and power budget are no less important than the knowledge of how to manipulate nitride optoelectronic properties.

The variety of techniques has been demonstrated for measuring the junction temperature in nitrides. The simplest one is the analysis of voltage versus current dependencies of a forward biased p-n junction<sup>2</sup>. Although indirect, this approach (temperature accuracy  $\pm 3^\circ\text{C}$ ) could be helpful, given that current and temperature distribution is uniform. The nematic liquid crystal thermography technique (the reflectivity of a probing polarised laser beam is affected by the temperature of a device surface covered with a set of nematic crystals with different transition temperatures) permits hot zone static profiling with a temperature resolution of  $1^\circ\text{C}$  (temperature accuracy  $4^\circ\text{C}$ , spatial resolution on the order of tens microns<sup>3,4</sup>). The temperature of an LED can be indirectly derived from the electroluminescence-photoluminescence emission

---

<sup>1</sup> E-mail: malyut@isp.kiev.ua

spectrum<sup>5,6</sup> (peak wavelength is connected to material bandgap and, thus, is a function of temperature) and Raman measurements<sup>7</sup> (the relative shift of the E<sub>2</sub>-phonon frequency under a current, when frequency at zero current is temperature sensitive value), permitting temperature accuracy no better than 10<sup>0</sup>C. In both cases, a spot diameter of ~1 μm permits record spatial resolution, while 2D- temperature mapping is a time consuming process.

In this paper we report on the study of heat 2D-distribution and local heat relaxation processes in flip-chip packaged InGaN blue LEDs performed with an IR microscopy technique that is operated in a time-resolved mode. While insufficient in spatial resolution due to diffraction limitation, this direct approach demonstrates high accuracy and extremely high measurement speed. The main stress is made on micro mapping of device overheating and local temperature gradients inside the structure. In particular, we show how current crowding (which is difficult to avoid), contact resistance, and problems connected to “hanging bridges” inevitably accompanying a flip-chip design, cause a local hot zone (heat traps) near the n-contact pad. We also show how local thermal resistance could affect the reliability and performance of a device at a high injection level. In addition, we discuss the reasons for dynamic (reversible) and static (irreversible) processes of device degradation.

## 2. EXPERIMENTAL

### 2.1. Device technology

The InGaN/GaN MQW heterostructures grown on sapphire substrates by metal organic chemical vapor deposition were used for fabrication of flip-chip LED dies. The structure consists of a 3 μm-thick Si-doped n<sup>+</sup>-GaN contact and current spreading layer, followed by InGaN/GaN MQW capped with ~200 Å-thick AlGaInN electron blocking layer. Finally, a 0.15 – 0.25 μm-thick Mg doped p-GaN is used as the upper contact layer. The In composition in MQW corresponds to the 460-470 nm emission wavelength. The post-growth processing includes standard photolithographic patterning, followed by a deep mesa etching down to the sapphire substrate and a shallow mesa etching to the n-CaN-cladding layer (Fig.1a). The rectangle-shaped 0.1 μ-thick reflective Ni/Ag/Ti/Au p-contact spreads the current over the structure and provides lower forward voltage. The “fork-like” Ti/Al/Ti/Au n-contact surrounds a rectangular 470 x 350 μm p-contact from three sides by forming an emitting area of a device comparable to the p-contact size. Both contacts are deposited by a magnetron sputtering and thermal vacuum evaporation. The LED structure is soldered in a flip-chip manner to the Si submount (Fig.1b), resulting in favorable conditions for heat removal (the distance between p-n junction and solder pad on the Si submount is less than 0.5 μm). Due to high reflectivity of a p-contact, downward propagating light is redirected toward the sapphire substrate with a chance to escape the chip, increasing light extraction. Finally, this structure is attached to a massive copper heat sink and electrical connections to the LED are made via the Si submount. The LED with a heat sink operates in a current range up to 800 mA (dissipated power up to 4 W). At 20 mA CW bias current the device exhibits 20-22% external quantum efficiency and 12 mW output power, whereas the maximum value of power emitted exceeds 200 mW.

### 2.2. Experimental setup

Although conventional thermal imaging systems permit direct high-speed mapping of heat distribution, these devices monitor IR signals emitted by an object with dimensions well beyond 100 μm. To map a heat pattern in tiny blue LEDs, we developed a micro-mapping system<sup>8</sup>, which consists of an IR reflection microscope co-axially attached to a calibrated scanning IR thermal imaging camera that is operated in 3–5 μm band range with MCT cooled photodetector (Fig.2). This spectral range permits spatial mapping of backside heat emission through a thin transparent sapphire substrate with spatial resolution of <20 μm, temperature resolution, and accuracy of 0.1<sup>0</sup>C and 0.5<sup>0</sup>C, respectfully. In this arrangement, the setup is insensitive to actual light emitted by blue LEDs.

The exposition time varies from 50–400 μs (single-line duration, heat profile) to 40 ms (full-frame duration, 2D-heat map), while the minimum time-resolved interval is 10 μs. The setup permits real-time study of the dynamic map with a recording 25 frames/s and production of a TV-like false color image. Data acquisition and image processing (emissivity equalization, noise reduction by image averaging, external triggering) are computer-controlled. A parallel video channel equipped with a CCD camera permits easy positioning and focusing of a <1×1mm<sup>2</sup> object and maps 2D- distribution of light emitted in the spectral range above 1 μm.

Significantly of note is that the IR thermal imaging camera measures radiance pattern but not temperatures. Therefore, apparent temperature  $T_a$  and power emitted  $P$  values are connected by a calibrated signal transfer function, whereas getting the real object temperature demands for a so-called emissivity correction procedure. Non-corrected thermal image of a device ( $I=0$ , case temperature  $50^{\circ}\text{C}$ ) is shown in Fig.1c. Because emissivity values of metals and semiconductors are different, this image permits an easy location of hot zones on the surface of a biased ( $I>0$ ) LED later.

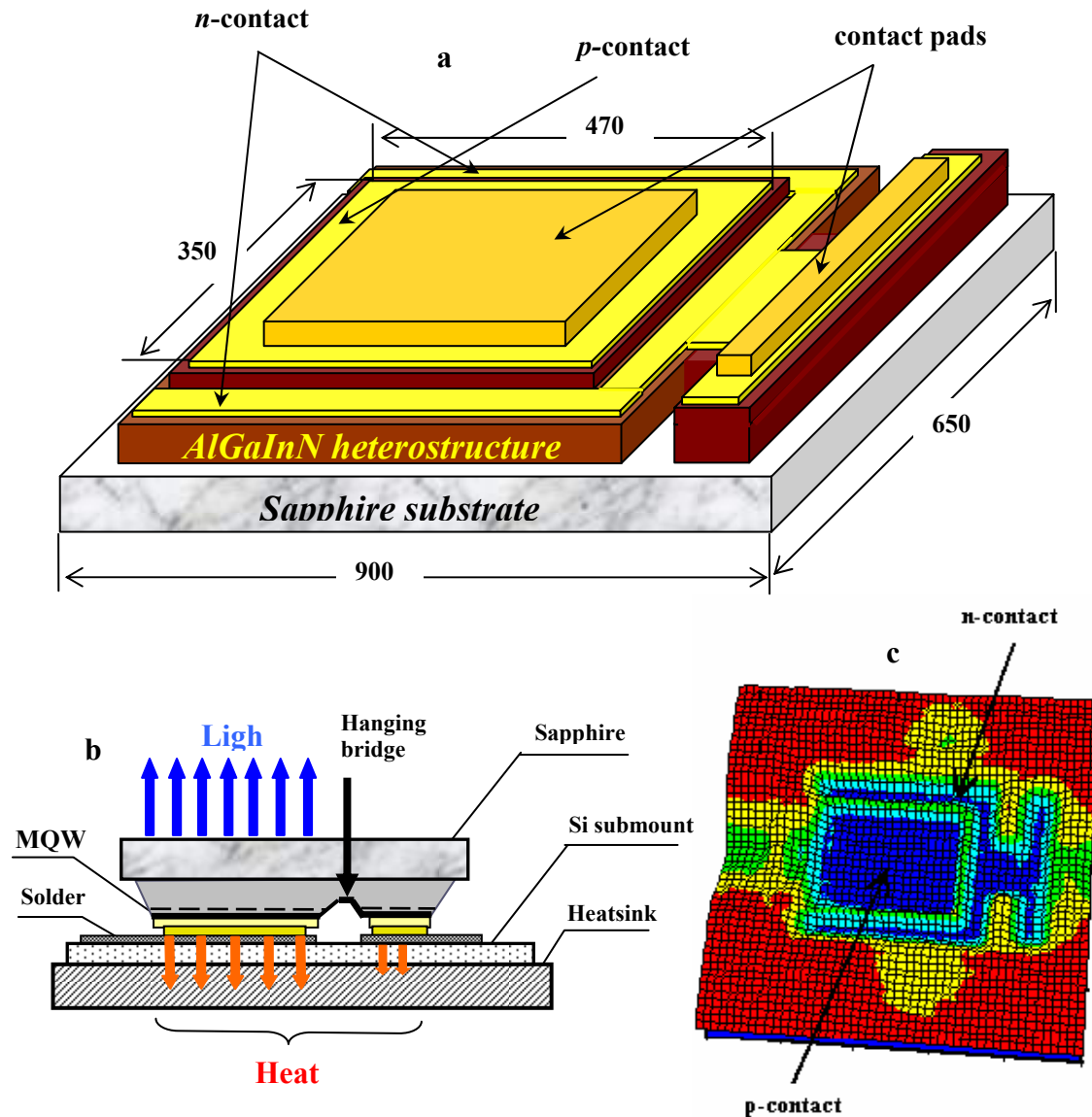


Fig.1. (a) A general view of a mesa structure (the dimensions are shown in microns), schematic cross section view of the “flip-chip” LED attached to a heat sink (b), and nonbiased device emissivity map captured through sapphire substrate (c).

The camera is synchronized with a current bias pulse ( $I$ ) in such a manner that a heat “picture” appears at the second frame  $T(I)$ , while the first frame captures the background (zero-biased) image  $T(0)$ . By subtracting these frames one can get a dynamic heat map provoked by a bias current,  $\Delta T = T(I) - T(0)$ . Besides, the setup permits heat relaxation study when the local temperature is measured with a given delay after a current pulse is turned off. In one word, the technique can provide information related to three dimensions- two spatial dimensions and time.

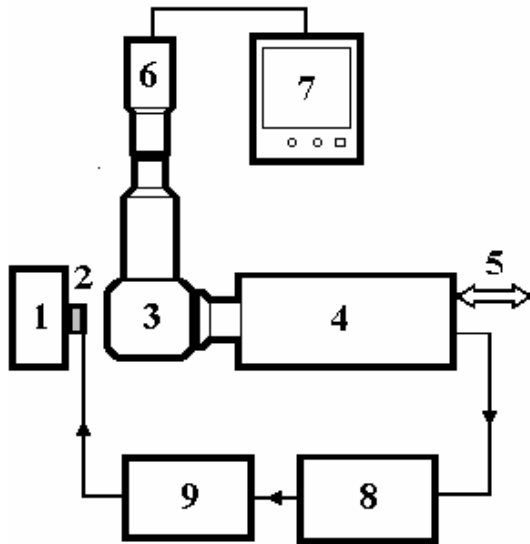


Fig.2. IR microscope experimental set up  
 1-positioning and heating stage, temperature controller;  
 2-LED under test;  
 3-IR reflective-type microscope;  
 4-thermal imaging scanning camera, 3-5  $\mu\text{m}$ ;  
 5 - computer control;  
 6- CCD camera,  
 7- monitor for visual positioning;  
 8- slave mode-operation unit;  
 9- bias current source.

### 3. RESULTS AND DISCUSSION

#### 3.1. 2D-heat distribution

The experiment shows that at  $I \leq 100$  mA the active area of the device practically does not suffer of Joule heating in CW mode. Indeed, the junction-to-case overheating in the flip-chip design is as low as  $\Delta T < 6$   $^{\circ}\text{C}$ . Moreover, this heat distributes uniformly over the all junction area and, thus, can be neglected. Still, this is not the case at a higher current; therefore, getting acceptable power emitted demands for a pulse mode operation. As an example, Fig.3a illustrates a typical heat pattern across an active area of the device at 160 ms pulse duration and 25 Hz repetition rate ( $I=200$  mA, the setup operates in a standard full-frame mode). Due to low heat dissipation time constant, these bias conditions permit easy localizing of the heat sources.

Indeed, heat maps systematically demonstrate hot regions, the geometry of which is strongly connected to contact positions. As a matter of fact, while comparing Fig.1c and Fig.3a, two hot regions are clearly positioned. Firstly, peripheral excess heat generates well beyond the emitting structure and strictly reproduces fork-like geometry of the n-contact. Secondly, and most important, more intense heat appears inside the emitting structure itself. This hot region follows contact geometry only slightly but mostly appears opposite to the central part of the n-contact. Both hot regions are separated by the “hanging bridge” that is created by the mesa etching process.

#### 3.2. 1D-dynamic heat profiling

Temperature profiles across an LED surface shown in Fig.3b give a deeper inside knowledge into the “anatomy” of hot regions. The profiles cross a device along three fixed lines shown in Fig.3a. Because of a higher current value ( $I=800$

mA), shorter pulse duration (the setup operates in the 400  $\mu$ s single-line mode), and ability to integrate the images, we have an excellent view of the heating process as well as its better spatial resolution.

The most striking effect the line-scan mode demonstrates is the existing of two symmetric heat traps inside the emitting area, which are represented by the saddle profiles in Fig.3b. Although the non-monotonic behavior is typical to all temperature profiles measured, remarkable heat bottlenecks appear in the vicinity of the crossbar of a contact fork, where local excess temperature jumps up to  $\Delta T \sim 50^\circ\text{C}$ . Even though this overheating looks quite acceptable from a common point of view, our estimates show that temperature gradients that this local heat develops exceed a stunning value of  $\Delta T/\Delta x > 7 \cdot 10^3 \text{ }^\circ\text{C}/\text{cm}$ .

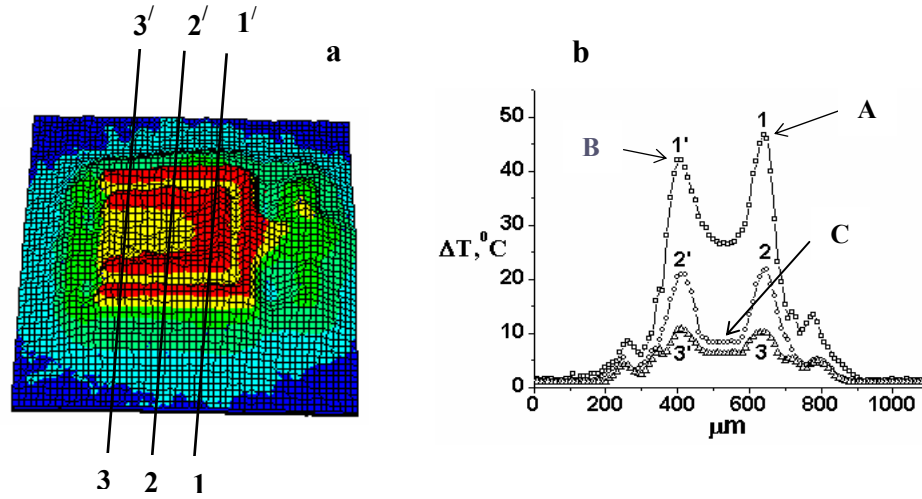


Fig.3. (a) IR image of excess temperature 2D-distribution captured through sapphire substrate at  $I=200$  mA and pulse duration 160 ms (full-frame mode, 4 frame averaging,  $\Delta T^{\text{max}}=9.5 \text{ }^\circ\text{C}$ ). (b) Excess temperature profiles at  $I=800$  mA and 400  $\mu$ s pulse duration (single-line mode, 64 - frame averaging, 10  $\mu$ m lateral step).

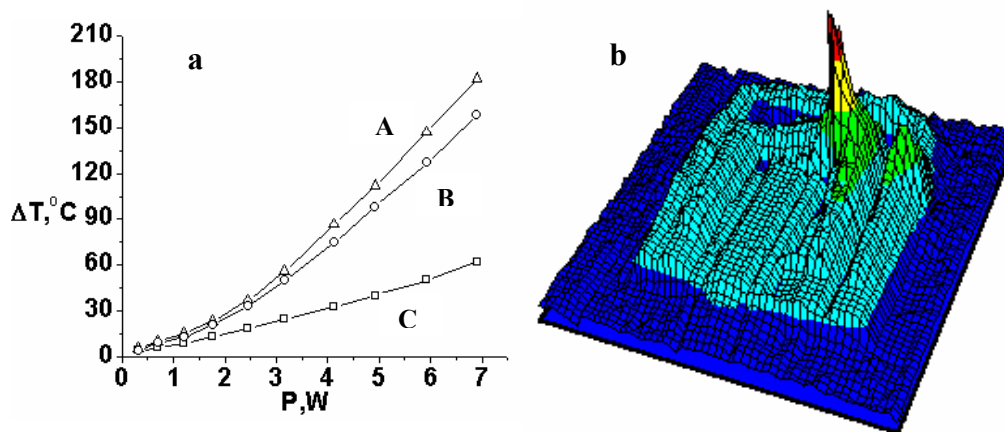


Fig.4. (a) Measured local overheating of three zones (shown in Fig.3b) plotted versus electrical drive power. Pulse duration 160 ms (full-frame mode, four - frame averaging). (b) Measured local overheating of degraded device at  $I=200$  mA ( $P=0.95$  W) and pulse duration 160 ms (full-frame mode, four- frame averaging) is as high as  $\Delta T=160 \text{ }^\circ\text{C}$ .

### 3.3. Static device degradation

It is taken for granted that blue LEDs efficiency degrades with increasing junction temperature. This type of degradation is caused by the interplay of radiative and nonradiative recombination processes and non-uniform current distribution as well. This dynamic degradation results in a temporary decrease of local efficiency and could be considered as a reversible process (being cooled a device recovers). However, relatively little is known about the irreversible or static LEDs degradation (catastrophic device failure) until recently. Shown in Fig.4a is an IR image of the structure captured after multiple cycling with 400  $\mu$ s-long multiple bias pulses ( $I = 1$  A). This “tired” device emits <10% of its initial power in blue but demonstrates local super overheating in the corner of the emitting area. As a matter of fact, this degraded device emits in IR like a point source due to local Joule heating of a degraded junction.

### 3.4. Lessons to learn

1) When it comes to excess heat in blue LEDs we face two reasons of concern. The problem of minor importance is in high series resistance of  $n^+$ -GaN current spreading layer and metallic fork-like n-contact. Although this contact is disclosed away from the emitting area (advantage of the flip-chip design!), its heating adds value to the wasted energy and drastically decreases the efficiency of the device. Also, this heat blocks the lateral diffusion of heat generated inside the active region of an LED. By an estimate, the resistance of a tiny n-contact strip ( $0.1 \times 50.0 \mu\text{m}^2$ ) is in the order of 3.0 Ohm, what results in a remarkable value of dissipated power at an extreme mode. This contact resistance also prevents the current to spread along a device area (compare heat profiles 1-1' and 3-3' shown in Fig.3b) and indirectly results in light<sup>9</sup> and heat concentration at the crossbar of a contact fork.

2) The reason of designer's concern should be the two symmetrical hot traps that we detected inside the emitting area. This local heat originating from an unavoidable current crowding in conventional mesa structures causes dynamic (thermally limited light power saturation) and static (catastrophic failure) device degradation. On the other side, there is room to learn the reason of static degradation. As we know, there could be two reasons. Firstly, the giant temperature gradient inside a multiple layer structure with different expansion coefficients could cause local irreversible mechanical stress of the p-n junction and provoke a catastrophic device failure<sup>10</sup>. Secondly, electrical and thermal effects combined could result in an activation of non-radiative recombination process through generation of active acceptors in p-GaN layer<sup>11</sup>.

3) The technology of blue LEDs integral testing can be hard to determine real device parameters by using integral testing of the devices. Indeed, our tests show that temperature distribution due to self heating effect scatters in a wide range ( $60^\circ\text{C} < \Delta T < 200^\circ\text{C}$ , see Fig. 4a), resulting in confused attempts to determine device properties integrally.

## 4. CONCLUSION

To summarize, in spite of impressive demonstration of last generation blue LEDs, it has become apparent that conventional flip-chip mesa structures grown on insulating sapphire substrates cannot provide many of requirements for high power devices, from which getting good reliability remains the most serious task. The drawback is that troubles arise with “hanging bridges” accompanying flip-chip design and lateral current crowding localized at the same place along the perimeter of p-contact. As a matter of fact, we need to introduce new technology, which typically means higher power dissipation. From this point of view, any attempt to develop additional path for current passing the device vertically looks challenging<sup>12</sup>

## REFERENCES

1. A. Chitnis, J. Sun, V. Mandavilli, R. Pachipulusu, S. Wu, M. Gaevski, V. Adivarahan, J. P. Zhang, M. Asif Khan, A. Sarua and M. Kuball, "Self-heating effects at high pump currents in deep ultraviolet light-emitting diodes at 324 nm", *Appl. Phys. Lett.* 81, 3491-3493, (2002).
2. Y. Xi and E. F. Schubert, "Junction-temperature measurement in GaN ultraviolet light-emitting diodes using diode forward voltage method", *Appl. Phys. Lett.* 85, 2163-2165, (2004).
3. Jeong Park, Moowhan Shin, Chin C. Lee, "Measurement of temperature profiles on visible light-emitting diodes by use of a nematic liquid crystal and an infrared laser", *Optics Letters* 29, 2656-2658, (2004).
4. Chin C.Lee, Joeng Parck "Temperature measurement of visible light-emitting diodes using nematic liquid crystal thermography with laser illumination", *IEEE Photonic Thech. Lett.* 16, 1706-1708, (2004).
5. Peter Fischer, Jurgen Christen, Margit Zacharias, Veit Schwegler, Chistoph Kirchner, Markus Kamp, "Direct imaging of the spectral emission characteristic of an InGaN/GaN-ultraviolet light-emitting diode by highly spectrally and spatially resolved electroluminescence and photoluminescence microscopy", *Appl. Phys. Lett.* 75, 3440-3442, (1999).
6. Y.Xi, J-Q.Xi, Th.Gessmann, J.M.Shah, J.M.Kim, E.F.Schubert, A.J.Fischer, M.H.Crawford, K.H.A.Bogart, A.A.Allerman, "Junction and carrier temperature measurement in deep-ultraviolet light-emitting diodes using three different methods", *Appl.Phys.Lett.* 86, 1907-1909, (2005).
7. Veit Schwegler, Matthias Seyboth, Sven Schad, Marcus Scherer, Cristoph Kirghner, Markus Kamp, Ulrich Stempfle, Wolfgang Limmer, and Rolf Sauer, "MRS Internet J. Nitride Semiconductor Res., 5S1, F99W11.18, (2000)
8. V. K. Malyutenko."High resolution 'vision' of dynamic electron processes in semiconductor devices", *Mat. Res. Soc. Simp. Proc.* 744, M4.10.1-M. 4.10.6, (2003).
9. W. H. Sun, J. P. Zhang, V. Adiravahan, A. Chitnis, M. Shatalov, S. Wu. Mandavilli, J. W. Yang, and M. A. Khan, "AlGaIn-based 280 nm light-emitting diodes with continuous wave powers in excess of 1.5 mW", *Appl. Phys. Lett.* 85, 531-533, 2004.
10. V. K. Malyutenko, O. Yu. Malyutenko, A. Dazzi, N. Gross, and J.-M. Ortega, "Heat transfer mapping in 3-5  $\mu$ m light emitting structures", *Appl. Phys. Lett.* 93, 9398-9340, (2003).
11. M. Pavesi, M. Manfredi, G. Meneghesso, S. Levada, E. Zanoni, S. Du and I. Eliashevich, "Optical evidence of an electrothermal degradation of InGaIn-based light-emitting diodes during electrical stress", *Appl. Phys. Lett.* 84, 3403-3405, (2004).
12. D. A. Zakheim, A. L. Zakheim, I. P. Smirnova, S. A. Gurevich V. W. Lundin, E.M.Arakcheeva, M.M.Kulagina, I.V.Rozhansky, A.F.Tsatsulnikov, A.V.Sasharov, A.V.Fomin, E.D.Vasil'eva, G.V.Itkinson, "Fabrication of high power flip-chip blue and white LEDs operating under high current density" *Phys.stat. sol.(c)*1, 2401-2404, (2004).